Biotechnology Advances 30 (2012) 142–153

Contents lists available at ScienceDirect

Biotechnology Advances

journal homepage: www.elsevier.com/locate/biotechadv

Computational model of EGFR and IGF1R pathways in lung cancer: A Systems Biology approach for Translational Oncology

Fortunato Bianconi [a,*], Elisa Baldelli [b], Vienna Ludovini [b], Lucio Crinò [b], Antonella Flacco [b], Paolo Valigi [a]

[a] Department of Electronic and Information Engineering, Perugia University, Italy
[b] Division of Medical Oncology, S. Maria della Misericordia Hospital, Perugia, Italy

ARTICLE INFO

Available online 18 May 2011

Keywords:
Systems Biology
Translation Oncology
EGFR
IGF1R
Mathematical modeling
Survival analysis

ABSTRACT

In this paper we propose a Systems Biology approach to understand the molecular biology of the Epidermal Growth Factor Receptor (EGFR, also known as ErbB1/HER1) and type 1 Insulin-like Growth Factor (IGF1R) pathways in non-small cell lung cancer (NSCLC). This approach, combined with Translational Oncology methodologies, is used to address the experimental evidence of a close relationship among EGFR and IGF1R protein expression, by immunohistochemistry (IHC) and gene amplification, by in situ hybridization (FISH) and the corresponding ability to develop a more aggressive behavior. We develop a detailed in silico model, based on ordinary differential equations, of the pathways and study the dynamic implications of receptor alterations on the time behavior of the MAPK cascade down to ERK, which in turn governs proliferation and cell migration. In addition, an extensive sensitivity analysis of the proposed model is carried out and a simplified model is proposed which allows us to infer a similar relationship among EGFR and IGF1R activities and disease outcome.

1. Introduction

Cancer is too complex a disease to be solely and completely described by the existing clinical variables (e.g., age of patient, size of tumor, histological grade, etc.) currently used in practice. It is therefore necessary to identify new biomarkers which will provide additional information about the cancer type, origin, or aggressiveness.

The behavior of genes and protein expression, and their relationships are the keys to investigate cancer cell response and their ability to proliferate, even if they are under drug effect. Systems Biology, together with Translational Oncology, could lead to a new approach to discover sensitive pathways in specific cancer cells that can be attacked by specific drugs, and a strategy to increase the possibility to have a positive response in the classes of cancer that, at the present state of the art, are insensitive to classic chemotherapy (Lazebnik, 2002; Gonzalez-Angulo et al., 2010).

Among tumors, lung cancer is the leading cause of cancer-related mortality in both men and women throughout the world. Most lung carcinomas are diagnosed at an advanced stage, leading to a poor prognosis. Lung cancers are generally divided into small cell lung cancer (SCLC) and non-small cell lung cancer (NSCLC). Non-small cell lung cancer accounts for approximately 85% of all lung cancers and its high mortality is mainly ascribed to disease recurrence after curative lung resection and the lack of effective treatment for advanced disease. Despite recent advances in treatment for the disease, a clearer understanding of the molecular interactions is still necessary. Therefore, targeting specific molecular signaling pathways involved in tumor development and progression remains the principal promising approach in the management of NSCLC.

In this paper we propose a Systems Biology approach combined with a Translational Oncology study to understand the molecular biology of the Epidermal Growth Factor Receptor (EGFR, also known as HER1/ErbB-1) and type 1 Insulin-like Growth Factor (IGF1R) pathways in NSCLC. EGFR and IGF1R pathways play a key role in various human cancers and are crucial for tumor transformation and survival of malignant cells. High EGFR and IGF1R expression and activity has been associated with multiple aspects of cancer progression including tumorigenesis, metastasis, resistance to chemotherapeutics and other molecularly targeted drugs (Blakesley et al., 1997; Dufourny et al., 1997; Khandwala et al., 2000; Gong et al., 2009; Varella-Garcia et al., 2009; Gualberto et al., 2010). In our previous study, we showed that IGF1R protein expression by immunohistochemistry (IHC) was associated with EGFR protein expression and high co-expression of both IGF1R and EGFR was a significant prognostic factor of worse disease free survival (DFS) in early stage NSCLC patients (Ludovini et al., 2009). These data could suggest a dynamic interaction between these two receptors. Starting from this data we built a computational model for EGFR and IGF1R pathways and we performed time behavior and sensitivity analysis under EGFR and IGF1R co-expression. The predictions of the model are verified by updating survival for IHC experiments and performing FISH experiments in the same population of NSCLC patients.

* Corresponding author.
E-mail address: fortunato.bianconi@diei.unipg.it (F. Bianconi).

0734-9750/$ – see front matter © 2011 Elsevier Inc. All rights reserved.
doi:10.1016/j.biotechadv.2011.05.010

1.1. Biological background

1.1.1. EGFR and IGF1R pathways

EGFR belongs to the HER/ErbB family of ligand-activated receptor tyrosine kinases (RTKs) which in addition includes: HER2 (ErbB-2/neu), HER3 (ErbB-3) and HER4 (ErbB-4) (Mendelsohn and Baselga, 2006; Scaltriti and Baselga, 2006). Members of the HER family are characterized by three main domains: an extracellular domain that is involved in ligand binding and receptor dimerization, a single transmembrane domain and a cytoplasmatic tyrosine kinase domain (Mitsudomi and Yatabe, 2010). EGFR can be activated by binding to different ligands including epidermal growth factor (EGF), transforming growth factor (TGF-α), betacellulin (BTC), epiregulin (EPR) and amphiregulin (AR). Ligand binding to the extracellular domain leads to the receptor dimerization (formation of homodimers or heterodimers) and subsequent autophosphorylation of the receptor on multiple tyrosine residues in the intracellular domain of each monomer (Schlessinger, 2002). These phosphorylated tyrosines serve as specific binding sites for adapter proteins that lead to the activation of multiple signaling pathways including mitogen-activated protein kinase (MAPK) and phosphatidylinositol-3-kinase (PIK3) (Yarden, 2001; Citri et al., 2003).

Similar to the HER family members, IGF1R is a transmembrane tyrosine kinase receptor encoded by the IGF1R gene located on chromosome 15q25–q26 (Riedemann and Macaulay, 2006). IGF1R is a heterotetrameric protein consisting of two polypeptide chains (linked by disulfide bonds), each one with an extracellular α subunit containing the ligand binding domain and a β subunit that comprises the transmembrane and the tyrosine kinase domains (Jiang et al., 1999; López-Calderero et al., 2010). The binding of insulin-like growth factor 1 (IGF-1) and IGF-2 to the extracellular domain of IGF1R induces the receptor tyrosine kinase activity with resultant autophosphorylation at specific tyrosine residues (Becker and Yee, 2008). The phosphorylated receptor triggers the association of the Insulin Receptor Substrates (IRSs) and other adaptor proteins with the subsequent activation of the MAPK and PIK3 cascades (Jones, 1995; LeRoith et al., 1995).

Both activated EGFR and IGF1R trigger the signal transduction events including the MAPK and PIK3 pathways (Denley et al., 2005).

1.1.2. MAPK cascade

Mitogen-activated protein kinases (MAPKs) are serine/threonine kinases that mediate cellular activities including cell proliferation, differentiation, survival, death and transformation (Pearson, 2001). These cascades contain at least three protein kinases in series: a MAPK kinase kinase (MAPKKK), a MAPK kinase (MAPKK) and a MAPK (Gary and Johnson, 2002). Mammalian cells have different MAPKs: extracellular signal-regulated kinase (ERK1/2), p38 and c-Jun NH2-terminal kinase (JNK). In this paper we will focus on the ERK pathway which plays an important role in several steps of tumor development (Kim and Choi, 2010).

Activation of both EGFR and IGF1R leads to the association of cytoplasmatic adaptor proteins including Grb2, Shc, Crk and p85 which recruit the guanine nucleotide exchange factor SOS-1 (Son Of Sevenless) to the receptor complex. SOS stimulates the exchange of GTP for GDP on the small GTPase RAS which cycles between inactive guanosine diphosphate (GDP)-bound and active guanosine triphosphate (GTP)-bound conformations (Ras-GDP and Ras-GTP, respectively) (Boguski and McCormick, 1993; Shane Donovana and Bollagb, 2002; Qi and Elion, 2005). Furthermore, Ras protein is negatively regulated by GTPase activating proteins (GAPs), which stimulate intrinsic GTPase activity by stabilizing a high-energy transition state that occurs during the Ras-GTP hydrolysis reaction (Schubbert et al., 2007). Ras-GTP binds to Raf determining its activation. Also Ras can interact productively with many effectors, including Raf and PIK3.

Raf kinase activates MAPK/ERK kinase (MEK) which in turn activates ERK (Yoon and Seger, 2006). ERK kinase can phosphorylates both cytosolic and nuclear substrates, including numerous transcription factors. Their activation can lead to the expression of proteins required for cell proliferation and cell survival (Roberts and Der, 2007). Cytosolic substrates of ERK include several pathway components involved in ERK negative feedback regulation. Among these ERK phosphorylates p90 Ribosomal S6 kinase (p90′Rsk) which phosphorylates SOS causing SOS–Grb2 complex dissociation, and interferes with Ras activation. Another important negative regulator of the ERK cascade is protein phosphatase 2A (PP2A) (Dong et al., 1996; Frödin and Gammeltoft, 1999; Orton et al., 2009).

1.1.3. PIK3 pathway

PIK3s constitute a lipid kinases family which is able to phosphorylate the inositol ring of inositol phospholipids in the membrane (phosphatidylinositol-4,5-bisphosphate (PIP2)) to generate the second messenger phosphatidylinositol-3,4,5-triphosphate (PIP3), which activates downstream Akt (Bader et al., 2005).

Akt is a cytosolic kinase which has the ability to phosphorylate a wide variety of substrate proteins in order to perform its various functions in the cell. In particular, Akt promotes cell survival inactivating several pro-apoptotic proteins (including BAD, procaspase 9 and Forkhead (FKHR) transcription factors) (Vivanco and Sawyers, 2002; Hennessy et al., 2005). Furthermore, Akt can negatively regulate MAPK pathway through B-Raf phosphorylation activity in its amino-terminal regulatory domain (Guan et al., 2000).

2. Material and methods

2.1. Mathematical modeling

2.1.1. Modeling pathway interactions

The biological relationship between the proteins involved in EGFR and IGF1R pathways and the downstream MAPK and PIK3 networks has been modeled by means of a set of ordinary differential equations (ODEs) to study the time behavior of the overall system, and the functional interdependences among the receptors, the proteins and kinases involved. ODEs were integrated by Matlab *sundials* solver (Hindmarsh et al., 2005).

The overall biological networks studied are depicted in Fig. 1, and the biochemical reactions covered by the model are detailed in Table 1 (where the parameter k is specific for each reaction, and where the second column indicates the type of kinetic law, according to the discussion in the next subsection).

As an example of the approach, we consider the case of Ras activation by SOS. The corresponding complete reaction is given by:

$$SOS + Ras \underset{d_1}{\overset{a_1}{\rightleftharpoons}} SOS\text{–}Ras \xrightarrow{k_1} Ras^* + SOS, \tag{1}$$

where Ras^* represents the active form of protein Ras and SOS–Ras is the reaction intermediate. The reaction can be modeled through the following set of differential equations by a direct application of the law of mass action:

$$\frac{d[SOS]}{dt} = -a_1[SOS][Ras] + d_1[SOS\text{–}Ras] + k_1[SOS\text{–}Ras] \tag{2a}$$

$$\frac{d[Ras]}{dt} = -a_1[SOS][Ras] + d_1[SOS\text{–}Ras] \tag{2b}$$

$$\frac{d[SOS\text{–}Ras]}{dt} = +a_1[SOS][Ras] - d_1[SOS\text{–}Ras] - k_1[SOS\text{–}Ras] \tag{2c}$$

$$\frac{d[Ras^*]}{dt} = k_1[SOS\text{–}Ras] \tag{2d}$$

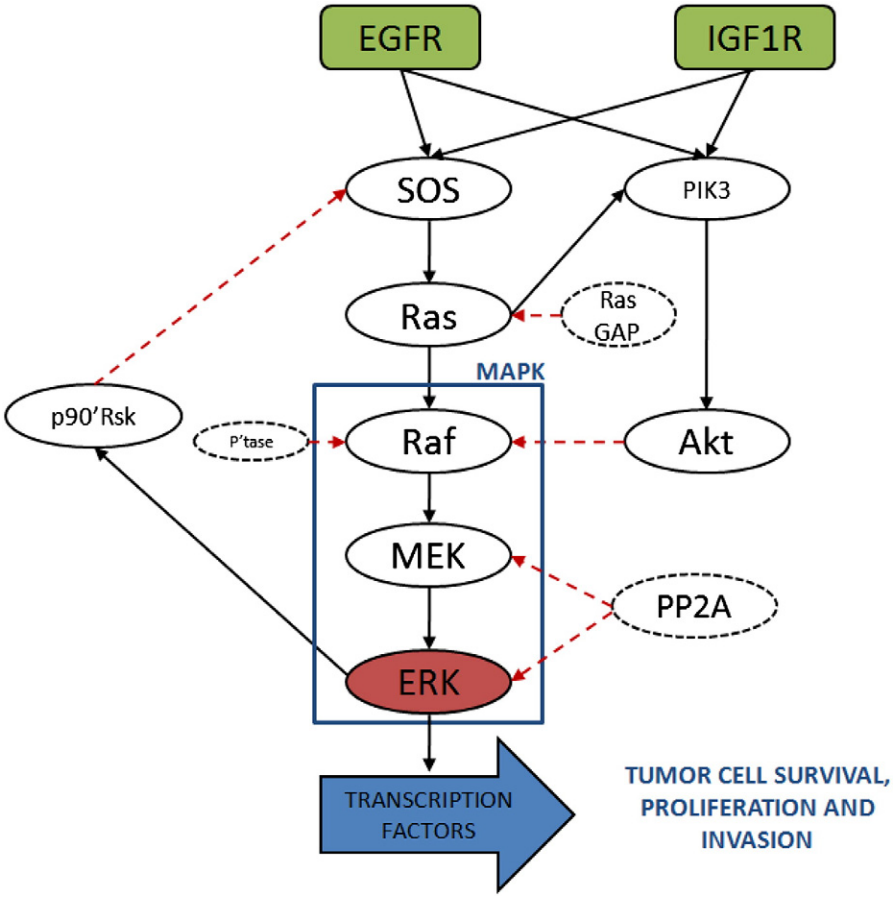

Fig. 1. Schematic of EGFR and IGF1R pathways.

where [S] denotes the concentration of substance "S". The above set of differential equations can be simplified by taking into account that, due to moiety conservation, the following constraints hold:

$$[SOS] + [SOS\text{–}Ras] = SOS_{tot} \tag{3a}$$

$$[Ras] + [SOS\text{–}Ras] + [Ras^*] = Ras_{tot}, \tag{3b}$$

Table 1
Model reactions and kinetic laws.

Kinetics reaction	Kinetic law
$EGFR^* + SOS \xrightarrow{k} SOS^* + EGFR^*$	EMM
$SOS^* + Ras \xrightarrow{k} Ras^* + SOS^*$	EMM
$p90Rsk^* + SOS^* \xrightarrow{k} SOS + p90Rsk^*$	EMM
$IGF1R^* + SOS \xrightarrow{k} SOS^* + IGF1R^*$	EMM
$PIK3CA + IGF1R^* \xrightarrow{k} PIK3CA^* + IGF1R^*$	EMM
$PIK3CA + EGFR^* \xrightarrow{k} PIK3CA^* + EGFR^*$	EMM
$Akt + PIK3CA^* \xrightarrow{k} Akt^* + PIK3CA^*$	EMM
$MEK^* + ERK \xrightarrow{k} ERK^* + MEK^*$	EMM
$Akt^* \xrightarrow{k} Akt$	Mass action
$ERK^* + PP2A \xrightarrow{k} ERK + PP2A$	EMM
$PIK3CA + Ras^* \xrightarrow{k} PIK3CA^* + Ras^*$	EMM
$Ras^* + Raf \xrightarrow{k} Raf^* + Ras^*$	EMM
$Raf^* + MEK \xrightarrow{k} MEK^* + Raf^*$	EMM
$Akt^* + Raf^* \xrightarrow{k} Raf + Akt^*$	EMM
$RasGap^* + Ras^* \xrightarrow{k} Ras + RasGap^*$	EMM
$PP2A + MEK^* \xrightarrow{k} MEK + PP2A$	EMM
$PIK3CA^* \xrightarrow{k} PIK3CA$	Mass action
$RafPP + Raf^* \xrightarrow{k} Raf + RafPP$	EMM
$p90Rsk + ERK^* \xrightarrow{k} p90Rsk^* + ERK^*$	EMM
$p90Rsk^* \xrightarrow{k} p90Rsk$	Mass action

where S_{tot} denotes total (and constant) concentration of substance "S". The detailed phosphorylation mechanism is described in (Markevich et al., 2004) through the same ODE approach, where there is evidence of the different dynamics arising from a processive or, respectively, distributive, dual phosphorylation and dephosphorylation.

An almost universally adopted approximation, which holds under steady-state assumptions for the intermediate (SOS–Ras in the above exemplification) consists in representing the rate of product formation by means of Michaelis–Menten kinetics. For our example, this is valid to assume the simplified reaction:

$$SOS + Rask \xrightarrow{k_1} Ras^* + SOS, \tag{4}$$

modeled by the following couple of differential equations:

$$\frac{d[Ras^*]}{dt} = k_1[SOS]\frac{[Ras]}{k_M + [Ras]} \tag{5a}$$

$$\frac{d[Ras]}{dt} = -k_1[SOS]\frac{[Ras]}{k_M + [Ras]}, \tag{5b}$$

where [SOS] is the enzyme concentration and k_M is the Michaelis constant. By simple algebraic computations starting from the complete model (2) it turns out that $k_M = (d_1 + k_1)/a_1$. Again, the above model could be reduced by taking into account that, in view of moiety conservation, $[Ras] + [Ras^*] = Ras_{tot}$. Also, notice that we are following the idea proposed in (Orton et al., 2009), to keep explicit the (possibly time-varying) enzyme concentration in the formulation of Michaelis–Menten kinetics. To this extent, the notation *EMM* in Table 1 refers to such a kinetic low.

The complete EGFR–IGF1R pathway studied in this paper can be modeled by following the above-outlined approach. The approach leads to the set of nonlinear ODEs given in Appendix *A1*.

As for the associated problem of parameter identification, among many other contributions, we mention the contribution (Bianconi et al., 2010) by some of the authors of this papers, as well as the references therein. Here, the focus is on the use of modeling on translation oncology, we make use of parameters mostly derived from the open literature, according to the Table 1.

2.1.2. Reduced model

In addition to the complete model described above, we also considered a simplified one, which allows for a quicker analysis of the effects of the interaction between the two pathway downstream EGFR and IGF1R receptors, respectively. Let X denote the aggregate signal transduction level of the pathway activated by (active) EGFR and Y the corresponding signal transduction level for IGF1R. Then, a simplified model to describe the interaction can be given by the following equations:

$$\dot{X} = A_X \frac{Y^{n_Y}}{\left(\Lambda_{XY}^{n_Y} + Y^{n_Y}\right)} U_X - \frac{X}{\tau_X} \tag{6a}$$

$$\dot{Y} = A_Y \frac{X^{n_X}}{\left(\Lambda_{YX}^{n_X} + X^{n_X}\right)} U_Y - \frac{Y}{\tau_Y} \tag{6b}$$

where A_X is the amplitude of the cross-activation of the component X by Y and A_Y is the amplitude of the cross-activation of the component Y by X, and U_X and U_Y denotes the expression level of active EGFR and IGF1R, respectively. The cross activations of either pathway are approximated through two non-linear Hill functions where n_X and n_Y give the cooperativities: for a very high value of n (in the order of 5 to 10) they approximate two corresponding Heaviside functions. The cross-talk function is triggered when the other component is greater than a certain threshold value (Λ_{XY}, Λ_{YX} respectively).

The maximum value reached by X and Y under the effect of the exogenous inputs (normalized to $U_X = U_Y = 1$) is given by $A_X\tau_X$ and $A_Y\tau_Y$, respectively. Using these values to rescale the levels of X and Y, and in particular rescaling time by the factor $\tau_X\left(\tau := \frac{t}{\tau_X}\right)$, and both input signals U_X and U_Y by $A_X\left(U_x = \frac{u_X}{A_X} \text{ and } U_y = \frac{u_Y}{A_Y}\right)$, reduces the number of free parameters in the model:

$$\dot{x} = \frac{y^{n_y}}{\lambda_1^{n_y} + y^{n_y}} u_x - x \tag{7a}$$

$$\dot{y} = \frac{1}{\varepsilon}\left(\frac{x^{n_x}}{\lambda_2^{n_x} + x^{n_x}}\right) u_y - \frac{1}{\varepsilon} y \tag{7b}$$

where $\lambda_1 = \frac{\Lambda_{XY}}{A_Y\tau_Y}$ and $\lambda_2 = \frac{\Lambda_{YX}}{A_X\tau_X}$ are the dimensionless cross-activation thresholds, and $\varepsilon = \frac{\tau_Y}{\tau_X}$, is the ratio of the time scales in the two pathways.

2.1.3. Sensitivity analysis

Sensitivity analysis is a tool that can be used to study the dependence of system behavior on model parameters. We refer to normalized dynamic sensitivities. For the i-th specie x_i with respect to a variation ∂k_j to the j-th parameter or specie k_j sensitivity is defined as:

$$S_{i,j}(t) := \frac{\partial x_i(t)}{\partial k_j}. \tag{8}$$

The normalized sensitivity is similarly defined as:

$$S_{ni,j} := \frac{k_j}{x_i(t)} S_{i,j}(t). \tag{9}$$

To give a synthetic indication of sensitivity level, in the following the maximum absolute value of the normalized sensitivity function over time will also be used:

$$S_{Mi,j} := \max_t |S_{ni,j}(t)|. \tag{10}$$

2.1.4. Phase planes, vector fields, and nullclines

For the case of a two-species network, the diagram of the vector $(x(t), y(t))$, as a parametric function of time t, is called the *phase plane*. At each point in the phase plane, the differential equations define a vector that tells us which direction and how far the dynamical system will move over the next small increment of time, Δt. This collection of vectors is called the *vector field*. A solution to the ODEs plotted in the phase plane is simply a curve that starts at some initial point (the initial conditions) and follows the vector field.

The vector field in the phase plane is conveniently characterized by the X- and Y-*nullclines*, i.e., by the curves for which the corresponding species' time derivative is exactly zero. Along the X-nullcline, the vector field points north or south because $\frac{dX}{dt} = 0$ (that is, no change in the east–west direction).

Similarly, along the Y-nullcline, the vector field points east or west because $\frac{dY}{dt} = 0$ (no change in the north–south direction). In the region between the nullclines, the vector field could show any direction. Wherever the nullclines intersect, the pair of ODEs have a steady state solution; i.e., the system exhibits an equilibrium point (both $\frac{dX}{dt} = 0$ and $\frac{dY}{dt} = 0$). Notice that an equilibrium point can be stable (upon species perturbation the system tends to restore the equilibrium values) or unstable (upon species perturbation the system definitely departs from the equilibrium values).

2.2. Experimental methods

2.2.1. Biological experiments

Tumors obtained from 130 patients who underwent complete surgical resection of primary NSCLC were evaluated for EGFR and IGF1R expression and gene amplification. The studied population was then followed in a specified follow-up program.

Paraffin-embedded sections from tumors obtained by surgery were collected for evaluated expression and gene amplification of both receptors by IHC and FISH analyses.

For IHC experiments, slides were incubated with IGF1R mouse antibody (clone 24–31) or with EGFR mouse antibody (clone 3147) and then IHC staining was evaluated utilizing a semiquantitative grading system. This system is based on four stages (0, no staining; 1+, staining in 1%–10% of considered cells; 2+, staining in 11%–25% of considered cells; 3+, staining in >25% of considered cells). A cutoff value of 10% positive cells was used in order to avoid inclusion of scattered positivity of the same intensity found in the normal bronchial tissue (Ludovini et al., 2009).

FISH assays were performed utilizing IGF1R custom probe and EGFR commercial probe. Gene amplification was valuated utilizing a semiquantitative grading system based on six stages. Each stage is created considering the increasing number of copies of the genes (disomy, low trisomy, high trisomy, low polisomy, high polisomy and gene amplification) and percentage of cells carrying at least 4 copies of the gene signals as described in (Varella-Garcia et al., 2009). Tumors were considered FISH positive when at least 10% of cells displayed at least 4 copies of the gene.

2.2.2. Statistical analysis for patient population

Disease-Free Survival (DFS) was defined as the time from diagnosis to first local, regional or distant recurrence; second primary malignancy or death from any cause, whichever came first. Patients who were alive and did not experience recurrence at the time of the analysis were censored at the last disease assessment date. Unless

otherwise specified, all tests are with 1 df. A probability value of ≤ 0.05 was considered as statistically significant. DFS and the 95% confidence intervals (CIs) were evaluated by the Kaplan–Meier method comparing the different groups by log-rank test. The Cox proportional hazards model was used to evaluate the prognostic role of each single studied parameter on DFS, in univariate and multivariate analyses (Ludovini et al., 2009).

3. Results

3.1. Model predictions

3.1.1. Time responses

We ran *in silico* experiments, i.e., we numerically integrated the equations reported in Appendix *A1*, and we obtained the time

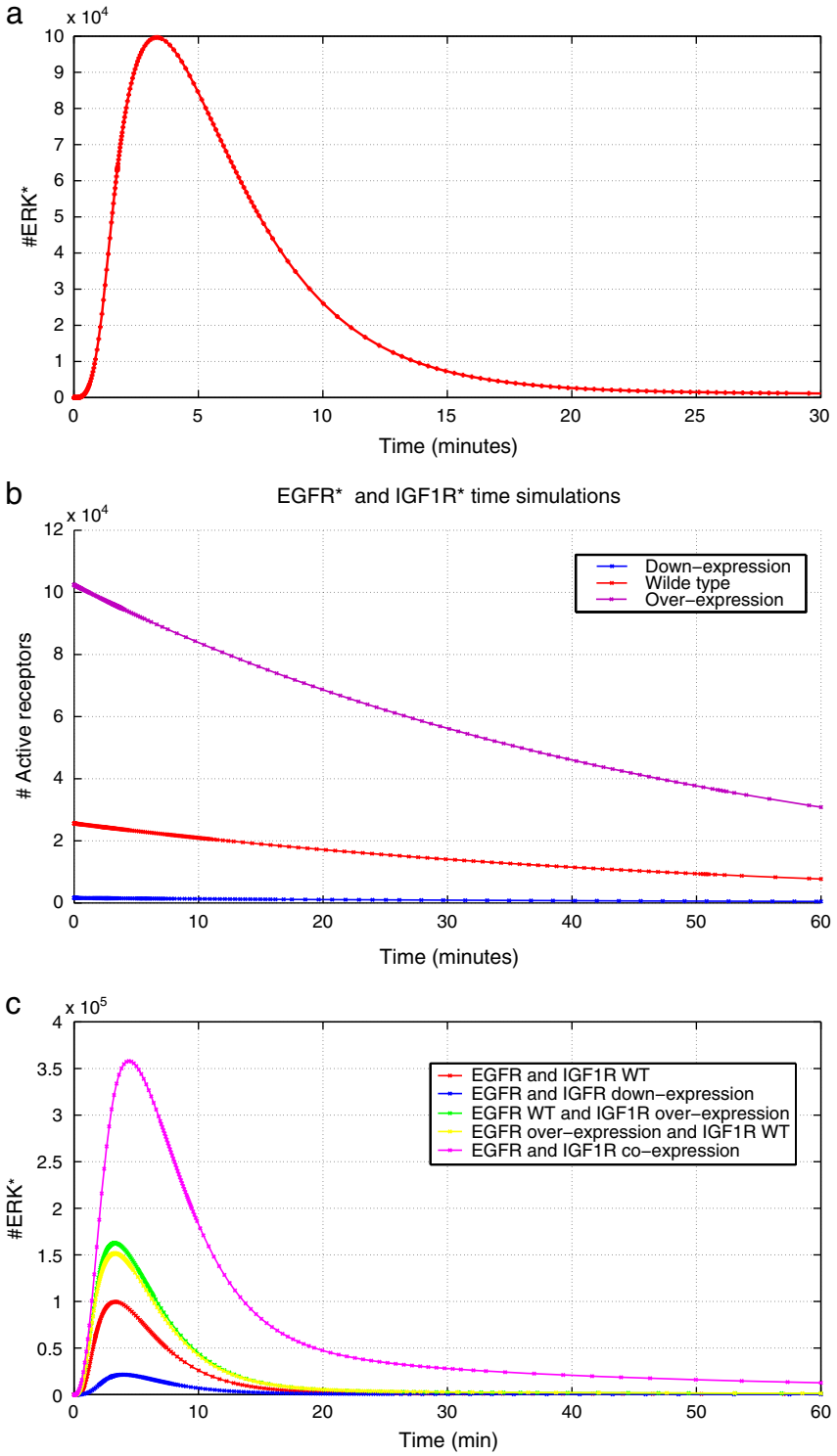

Fig. 2. Time response of the model. 2(a) Wild type *ERK** response. 2(b) EGFR and IGF1R receptors time responses under different initial conditions of the active form: wild type (red line), down expression (blue line) and over expression (magenta line). 2(c) *ERK** time response: wild type (red line), EGFR and IGF1R down expression (blue line), IGF1R over expression (green line), EGFR over expression (yellow line) and IGF1R and EGFR co-expression (magenta line).

evolution of all the species comprising the model. We focused on active ERK as the target to investigate signal transduction in tumor cells under EGFR and IGF1R stimulation. The qualitative shape of ERK is comparable with data in (Orton et al., 2009). As can be seen in Fig. 2(a), ERK is rapidly activated reaching a maximum at ~5 min and returning to basal levels at ~30 min.

We simulated four scenarios that reproduce typical EGFR and IGF1R receptor expression in NSCLC. To model the different scenarios, we properly selected initial values for the active forms of EGFR and IGF1R, as shown in Fig. 2(b). Such an approach is a way to model a quick variation on the concentration of the corresponding activated receptors. Hence, the initial conditions are not equilibrium values in that they described the receptor state immediately after the action of an external stimuli, which we assume as impulsive, for the sake of modeling simplicity. Fig. 2(c) compares ERK time response under wild type condition with receptors down expression (blue line), IGF1R over expression (green line), EGFR over expression (yellow line) and IGF1R and EGFR co-expression. The simulations suggest that there is a strong signal transduction when there is a high expression of both receptors.

3.1.2. Sensitivity analysis results

To explore the global system response from receptor expression to signal transduction we uniformly sampled the receptor space in a range from a minimum to a maximum expression level. We simulated the model for each set of parameter values and calculated the corresponding dynamic normalized sensitivities of *ERK** to *EGFR* and *IGF1R*, $(S_{ERK^*,EGFR}(t), S_{ERK^*,IGF1R}(t))$. Fig. 3 shows the maximum of *ERK** dynamic normalized sensitivities (i.e., the synthetic sensitivity S_M in Eq. (10)) at each point of the grid sampling for IGF1R and EGFR. The sensitivity of *ERK** to *IGF1R* increases while increasing the receptor's expression level (Fig. 3(a)). We found a similar behavior for *ERK** sensitivity to *EGFR* even if it is less strong than *IGF1R* (Fig. 3(b)). We also correlated the *ERK** dynamic normalized sensitivities to *EGFR* and *IGF1R*; there is a high correlation, almost ~1, for each set of parameter values as can be seen in Fig. 4.

3.1.3. Simulations for the reduced model

The nullclines in Fig. 5(a) (red and blue lines) show that the system is bistable; i.e., it has two asymptotically stable equilibrium points, at which both the signal transduction level *X* (referred to EGFR) and Y (related to IGF1R) have a high or low value, respectively. The third equilibrium point, characterized by intermediate values for aggregate signals *X* and *Y*, is unstable and cannot be experimentally observed.

If one disturbs the system from the stable equilibria characterized by a high expression of both aggregate signals (for example, a degradation due to some external factor to the model itself) the other equilibrium can be reached (Fig. 5(a)). This behavior is more evident for high cross-talk as shown in Fig. 5(b). The analysis suggests that a simple molecular mechanism may allow the system to switch from one functional state to another.

The above-mentioned dynamic properties of the cross-activation network, bistability and hysteresis, are invariant for a range of parameter values and molecular mechanisms at high values of n_x and n_y. That is, they are qualitative properties of the system. For instance, a moderate increase in the value of λ_1 and λ_2 causes the nullclines to move upwards. This deforms the phase portrait, but does not lead to the loss of the bistability and hysteresis properties, as long as the high value of cooperativities are maintained (see Fig. 5(d)). However, for low values of n_x and n_y, the qualitative properties may not be invariant. Fig. 5(c) shows that for values of $\lambda_1 = \lambda_2 = 0.7$ one of the stable equilibria and the unstable equilibrium annihilate each other, so that the system is no longer bistable and no longer exhibits hysteresis and we have a bifurcation condition (Bianconi, 2010).

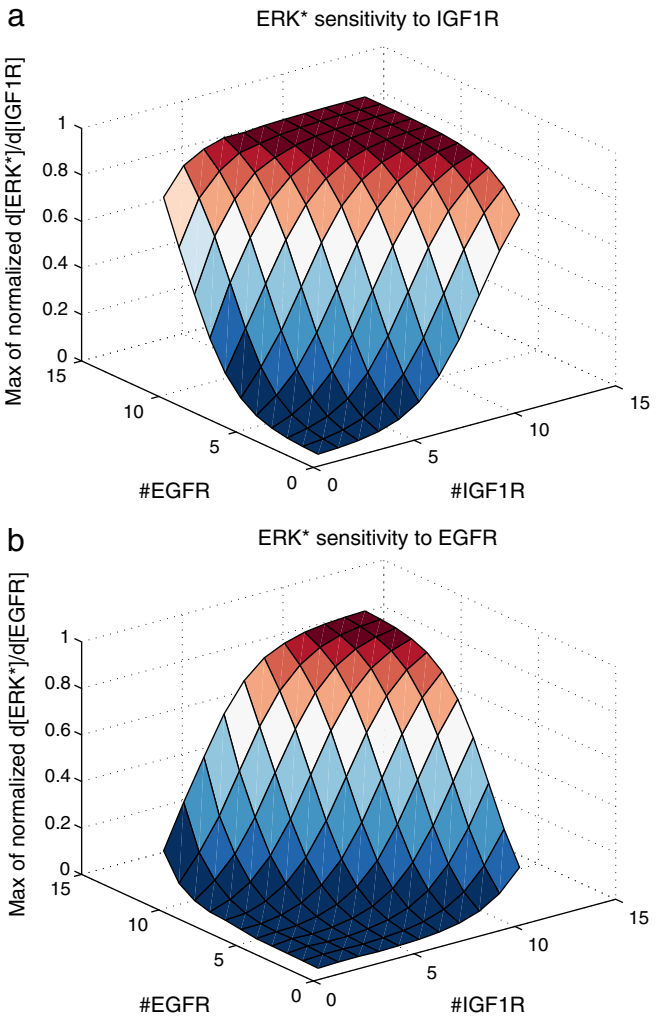

Fig. 3. Sensitivity analysis. 3(a) Maximum of $S_{n_{ERK^*,IGF1R}(t)}$ as function of *EGFR* and *IGF1R*. 3 (b) Maximum of $S_{n_{ERK^*,EGFR}(t)}$ as function of *EGFR* and *IGF1R*.

3.2. Experimental results

DFS was evaluated for NSCLC patients according to EGFR and IGF1R protein over-expression and gene amplification using the scores described in Sec. 2.2.1. Patients were divided into three groups: group I with protein expression of both receptors, group II with amplification of both genes and group III with both co-expression and co-amplification (Fig. 6). A difference in survival among these groups was described in the univariate analysis. The subset of patients with co-expression showed a worse DFS [25 months versus 90 months; hazard ratio (HR) 1.71, 95% CI 0.97 − 3.01, $P = 0.05$] when compared with the patients who had no co-expression. The Kaplan Meier survival estimates for this group is shown in Fig. 6(a). A statistically significant difference in DFS was observed between patients with gene co-amplification and patients who had no co-amplification (25 months versus not reached; HR 1.76; 95% CI 0.99 − 3.13, $P = 0.05$) (Fig. 6(b)). Also, a very significant shorter DFS is observed in the group III (10 months versus 85 months; HR 2.84; 95% CI 1.38 − 5.84 , $P = 0.005$) (Fig. 6(c)).

4. Discussion

Tumor development and progression are multi-step processes that require accumulation of several genetic alterations in a single cell.

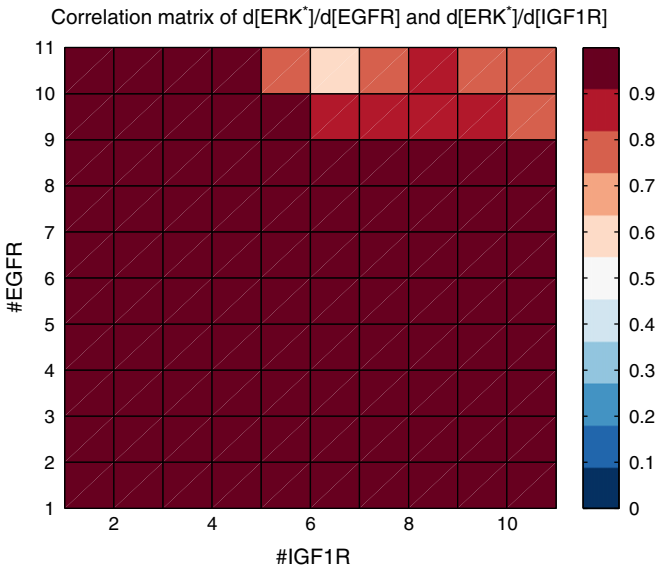

Fig. 4. Correlation matrix of $S_{n_{ERK^*,EGFR}(t)}$ and $S_{n_{ERK^*,IGF1R}(t)}$.

Understanding the molecular mechanisms involved in tumor development is an important goal of cancer prevention and treatment. In NSCLC the principal alterations now well-recognized have been found in the EGFR and IGF1R signaling pathways (Ludovini et al., 2009). There are a few mechanisms which lead to aberrant activation of receptors; these include: over-expression, gene amplification, mutations and over-expression of its ligands (Zandi et al., 2007; Gong et al., 2009; Dziadziuszko et al., 2010; Gualberto et al., 2010). Consequently, EGFR and IGF1R receptors have been intensively studied as therapeutic targets for NSCLC and so far the drug outcomes have been only partially successful. Furthermore, it is important to have a detailed molecular and genetic knowledge about the mechanisms leading to cancer development, to design new specific treatment approaches.

In this study we combined Systems Biology tools with Translational Oncology approaches in order to achieve a better understanding of the molecular mechanisms involved in tumor proliferation and to give a contribution to the development of more effective treatments.

Tumors obtained from surgical resection of primary NSCLC were evaluated for EGFR and IGF1R expression and gene amplification. IGF1R protein expression by immunohistochemistry was associated with EGFR protein expression. High co-expression of both IGF1R and EGFR was a significant prognostic factor of worse disease-free survival in early stage NSCLC patients. Co-expression of both EGFR and IGFR is associated with a worse disease-free survival (DFS) (Ludovini et al., 2009). Motivated by these clinical results, we built a mathematical model with the aim of analyzing pathway response to different expression levels of proteins.

To correlate EGFR and IGF1R expression level to tumor cell proliferation, we focused on the ERK signaling pathway, which plays

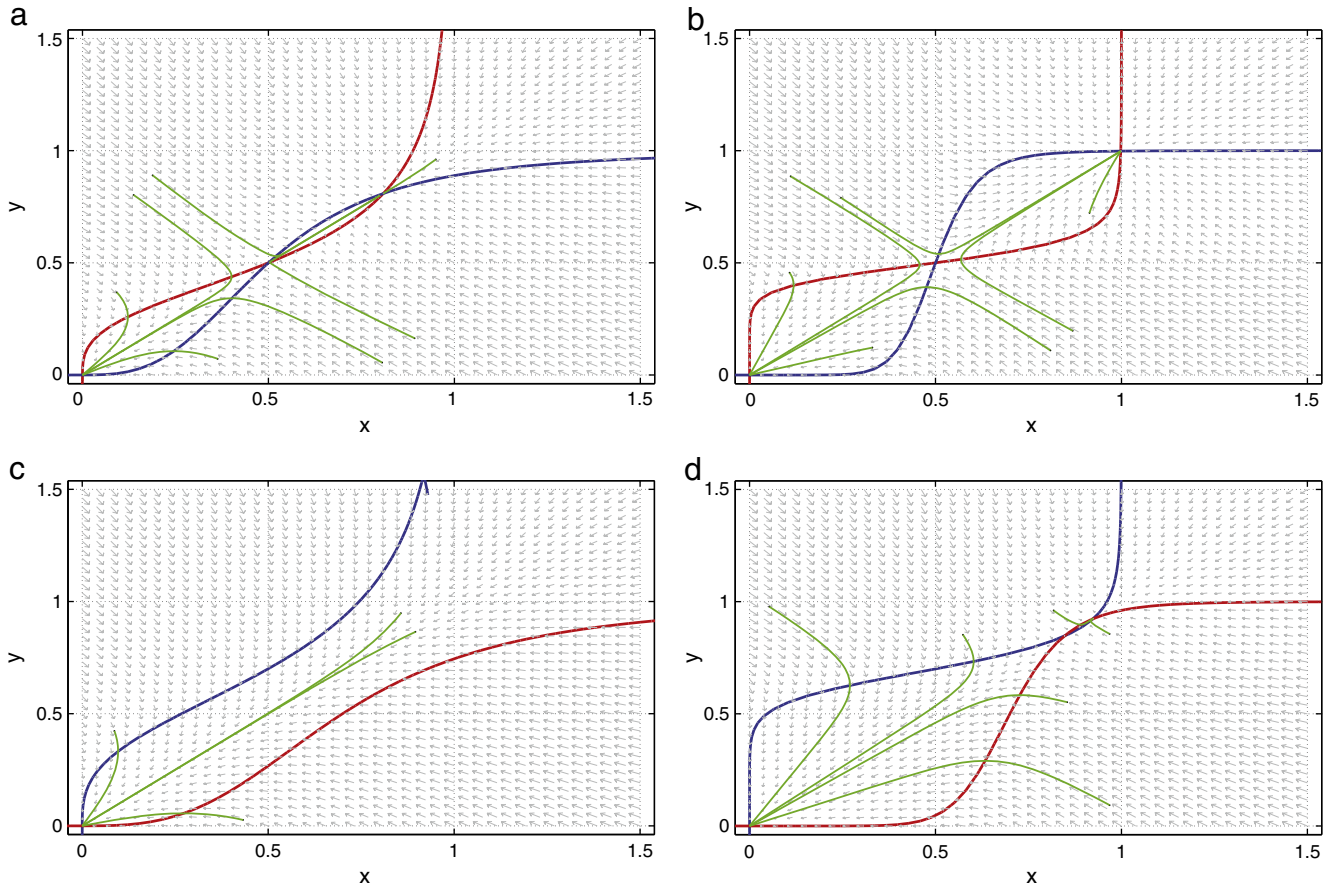

Fig. 5. Vector field (gray arrows), nullclines (red and blue line) and some trajectories for the reduced model (7a and 7b) (green line). Parameter values are $u_x = u_y = 1$, $\varepsilon = 1$ and we changed the cooperativities between the two pathways and the thresholds of the hysteresis. (a) $n_x = n_y = 3$ and $\lambda_1 = \lambda_2 = 0.5$. (b) $n_x = n_y = 9$ and $\lambda_1 = \lambda_2 = 0.5$. (c) $n_x = n_y = 3$ and $\lambda_1 = \lambda_2 = 0.7$. (d) $n_x = n_y = 9$ and $\lambda_1 = \lambda_2 = 0.7$.

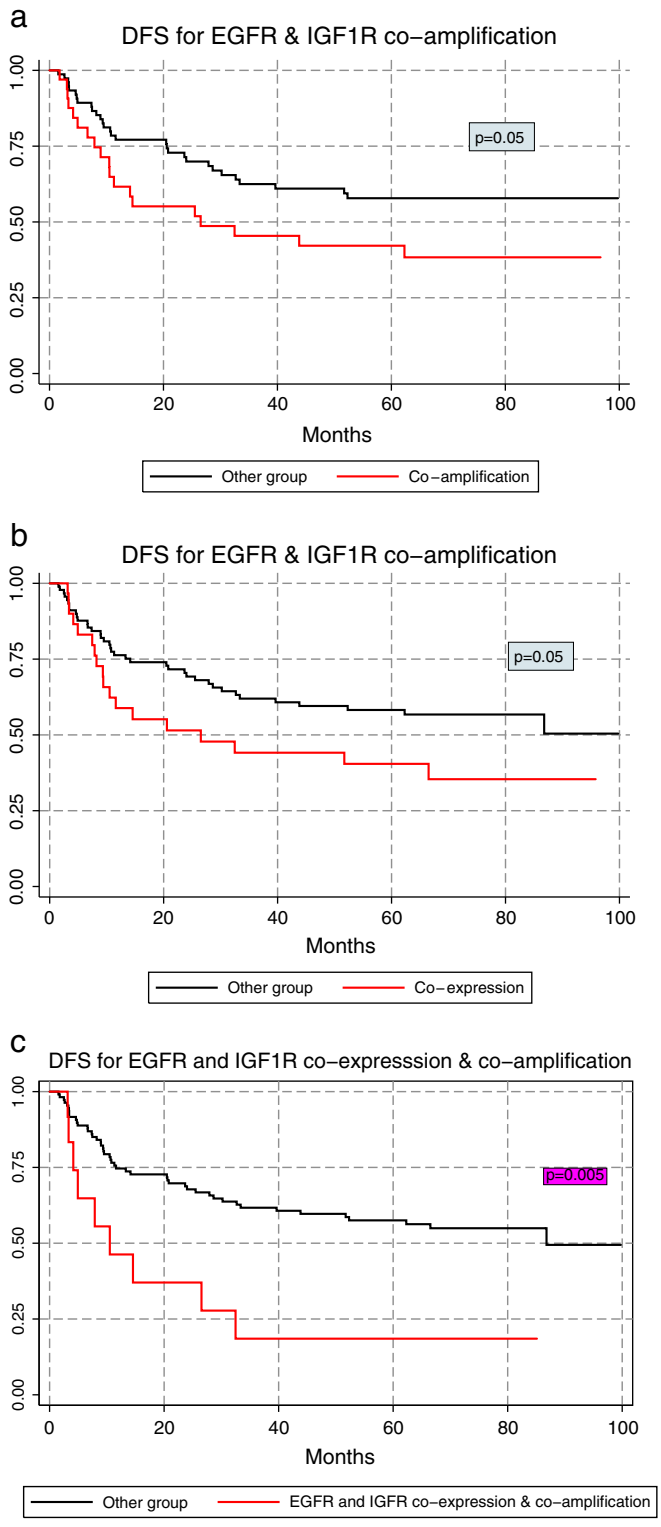

Fig. 6. Disease free survival (DFS). 6(a) Kaplan Meier estimates for DFS according to EGFR and IGF1R protein high expression. 6(b) Kaplan Meier estimates for DFS according to EGFR and IGF1R gene amplification. 6(c) Kaplan Meier estimates for DFS according to contemporary EGFR and IGF1R protein expression and gene amplification.

a central role in several steps of cancer development including proliferation and cancer cell migration (Kim and Choi, 2010). Cell proliferation can be closely related to the disease progression rate and therefore, in survival analysis, to DFS estimator.

We built a mathematical model describing the influence of EGFR ad IGF1R on the ERK signaling pathway. The EGFR/ERK pathway has been studied by several authors (Brown et al., 2004; Orton et al., 2009; Zielinski et al., 2009). They focused on the role of EGFR on the ERK-based outcome of the signaling pathway and (Orton et al., 2009) improved the previous model to cover receptor production and degradation as well as some additional pathways leading to ERK activation.

The approach proposed in this paper is similar to that of (Orton et al., 2009). Since our interest is in the impact of active receptor levels on ERK signaling, with respect to (Brown et al., 2004) and (Orton et al., 2009) we neglected the details of ligand–receptor interactions. At the same time, since we focused on the co-expression of EGFR ad IGF1R, we expanded the model to also cover the IGF1R pathway.

According to the scheme depicted in Fig. 1, and based on a modular modeling approach (as in (Bianconi, 2010)), we used the SOS complex to take into account all the adapter proteins; Ras to take into account the GTPase triggering the MAPK module and PIK3 in view of its relevance as a cytoplasmatic signaling pathway activated by both receptors (Sec. 1.1.1 and (Ludovini et al., 2011)); Akt as part of a negative regulation feedback; and finally the negative feedback of ERK on SOS mediated through p90′Rsk. The important issue of parameter estimation is not considered in this paper. Several approaches are available (see (Bianconi et al., 2010) and the references therein).

The *in silico* simulation of our model (see Fig. 2) clearly shows that the strongest modification on ERK time response behavior occurs when both EGFR and IGF1R have a high expression level. At the same time, over expression of EGFR or IGF1R alone gives rise to a lower impact on signal transduction. To model several expression levels of the two receptors, we simple used proper values of the corresponding initial conditions. Those conditions are not equilibrium ones, in that they describe the receptor activation levels immediately after the onset of external stimuli.

To further investigate the role of EGFR and IGF1R on ERK signaling and hence, on cell proliferation, we carried out a sensitivity analysis as described in Sec. 3.1.2. Fig. 3 shows that the system exhibits a low sensitivity both on EGFR and IGF1R whenever both receptors have a reduced expression level. Also, the analysis shows that the ERK signal has a maximum level of sensitivity to EGFR only if both receptors are over-expressed. Similarly, ERK sensitivity to IGF1R is high when both receptors are over-expressed. Such sensitivity results confirm the evidence from clinical data (see below) of a strong relationship between a simultaneous high expression level of both receptors and modification on ERK time behavior, which in turns implies a stronger attitude on cell proliferation.

An additional result derived through the model is the correlation between ERK sensitivity to EGFR and to IGF1R. The result, depicted in Fig. 4, shows that the two sensitivities are highly correlated, thus confirming again the clinical evidence.

The results achieved by means of the detailed model are confirmed by the simplified one as well, which shows that a positive cross-talk between the two pathways is a condition for signal transduction inside the tumor cell. However, the stable point in the phase plane near $(x, y) = (1, 1)$ is the condition where the external signal is propagated inside the cell and triggers a cascade of reactions that favor the growth and duplication of the tumor cell. When the IGF1R and EGFR active forms are low the model shows that the system is in stable equilibrium near $(x, y) = (0, 0)$: from a biological point of view this means that the cross-positive talk does not mediate the transduction of the signal, and therefore tumor cells grow slower than in the opposite condition. We can change the cooperativities and the thresholds to enlarge the convergence region of such a non-transducting equilibrium point in the origin.

For the same population studied in (Ludovini et al., 2009), we updated patients followed up and DFS according to IHC analysis. The mathematical model predictions seem to confirm clinical results as shown in Fig. 6(a). Patients with EGFR and IGF1R co-expression have a statistically significant shorter DFS ($p = 0.05$): this outcome can be related to high ERK activity in the mathematical model when both receptors have a high activity levels (Figs. 3, 5). We performed FISH analysis to understand the relationship between the gene and its protein levels. The group of patients who have an amplification of both genes presents a DFS comparable to the group with high expression of both proteins ($p = 0.05$) (Fig. 6(b)). Finally, group III (patients who had both co-expression and co-amplification) has a shorter DFS as shown in Fig. 6(c). This clinical result seems to suggest a correlation between high gene amplification and receptor activity and confirms the mathematical predictions of our model.

5. Conclusions

In this paper we propose a Systems Biology approach, combined with Translational Oncology methodologies, to understand the interaction between EGFR and IGF1R pathways in non-small cell lung cancer. The main objective of the paper is to address the experimental evidence of a close relationship between EGFR and IGF1R protein expression, gene amplification and the corresponding ability to develop a more aggressive behavior. We develop a detailed *in silico* model, based on ordinary differential equations, of the pathways. A simplified model is also proposed, which yields similar conclusions to the complete one. The results of the two models confirm the clinical evidence of a close relationship among receptor co-expression and ERK signaling alteration.

Funding

The work of EB, VL, AF, and LC was supported by a grant from the Italian Association for Cancer Research (AIRC) and from the Umbria Association Against Cancer (AUCC). The work of FB was supported by a fellowship from Fondazione Cassa di Risparmio di Perugia. The authors thank the patients who participated in this study.

Appendix

A1. Reactions and ODE's

The complete set of ODE's describing the model:

$$\frac{d}{dt}[EGFR^*] = -\gamma_{EGFR}[EGFR^*] - k_{SOS:E}[EGFR^*]\frac{[DSOS]}{KM_{SOS:E} + [DSOS]} - k_{PIK3:EGFR}[EGFR^*]\frac{[PIK3]}{KM_{PIK3:EGFR} + [PIK3]}$$

$$\frac{d}{dt}[IGF1R^*] = -\gamma_{IGF1R}[IGF1R^*] - k_{SOS:I}[IGFR^*]\frac{[DSOS]}{KM_{SOS:I} + [DSOS]} - k_{PIK3:IGF1R}[IGF1R^*]\frac{[PIK3]}{KM_{PIK3:IGF1R} + [PIK3]}$$

$$\frac{d}{dt}[SOS] = k_{SOS:E}[EGFR^*]\frac{[DSOS]}{KM_{SOS:E} + [DSOS]} + k_{SOS:I}[IGFR^*]\frac{[DSOS]}{KM_{SOS:I} + [DSOS]} - k_{DSOS:p90Rsk}[p90Rsk^*]\frac{[SOS]}{KM_{DSOS:p90Rsk} + [SOS]} - k_{Ras:SOS}[SOS]\frac{[Ras]}{KM_{Ras:SOS} + [Ras]}$$

$$\frac{d}{dt}[DSOS] = k_{DSOS:p90Rsk}[p90Rsk^*]\frac{[SOS]}{KM_{DSOS:p90Rsk} + [SOS]} - k_{SOS:E}[EGFR^*]\frac{[DSOS]}{KM_{SOS:E} + [DSOS]} - k_{SOS:I}[IGFR^*]\frac{[DSOS]}{KM_{SOS:I} + [DSOS]}$$

$$\frac{d}{dt}[Ras^*] = k_{Ras:SOS}[SOS]\frac{[Ras]}{KM_{Ras:SOS} + [Ras]} - k_{Ras:RasGab}[RasGab]\frac{[Ras^*]}{KM_{Ras:RasGab} + [Ras^*]} - k_{PIK3:Ras}[Ras^*]\frac{[PIK3]}{KM_{PIK3:Ras} + [PIK3]} - k_{Raf:Ras}[Ras^*]\frac{[Raf]}{KM_{Raf:Ras} + [Raf]}$$

$$\frac{d}{dt}[Ras] = -k_{Ras:SOS}[SOS]\frac{[Ras]}{KM_{Ras:SOS} + [Ras]} + k_{Ras:RasGab}[RasGab]\frac{[Ras^*]}{KM_{Ras:RasGab} + [Ras^*]}$$

$$\frac{d}{dt}[Raf^*] = k_{Raf:Ras}[Ras^*]\frac{[Raf]}{KM_{Raf:Ras} + [Raf]} - k_{Raf:RafPP}[RafPP]\frac{[Raf^*]}{KM_{Raf:RafPP} + [Raf^*]} - k_{Raf:Akt}[Akt^*]\frac{[Raf^*]}{KM_{Raf:Akt} + [Raf^*]} - k_{Raf:MEK}[Raf^*]\frac{[MEK]}{KM_{Raf:MEK} + [MEK]}$$

$$\frac{d}{dt}[Raf] = -k_{Raf:Ras}[Ras^*]\frac{[Raf]}{KM_{Raf:Ras} + [Raf]} + k_{Raf:RafPP}[RafPP]\frac{[Raf^*]}{KM_{Raf:RafPP} + [Raf^*]} + k_{Raf:Akt}[Akt^*]\frac{[Raf^*]}{KM_{Raf:Akt} + [Raf^*]}$$

$$\frac{d}{dt}[MEK] = -k_{MEK:Raf}[Raf^*]\frac{[MEK]}{KM_{MEK:Raf} + [MEK]} + k_{MEK:PP2A}[PP2A]\frac{[MEK^*]}{KM_{MEK:PP2A} + [MEK^*]}$$

$$\frac{d}{dt}[MEK^*] = +k_{MEK:Raf}[Raf^*]\frac{[MEK]}{KM_{MEK:Raf} + [MEK]} - k_{MEK:PP2A}[PP2A]\frac{[MEK^*]}{KM_{MEK:PP2A} + [MEK^*]} - k_{Erk:MEK}[MEK^*]\frac{[Erk]}{KM_{Erk:MEK} + [Erk]}$$

$$\frac{d}{dt}[Erk^*] = k_{Erk:MEK}[MEK^*]\frac{[Erk]}{KM_{Erk:MEK} + [Erk]} - k_{Erk:PP2A}[PP2A]\frac{[Erk^*]}{KM_{Erk:PP2A} + [Erk^*]} - k_{DSOS:Erk}[Erk^*]\frac{[SOS]}{KM_{DSOS:Erk} + [SOS]} - k_{EGFR:Erk}[Erk^*]\frac{[EGFR^*]}{KM_{EGFR:Erk} + [EGFR^*]}$$

$$\frac{d}{dt}[Erk] = -k_{Erk:MEK}[MEK^*]\frac{[Erk]}{KM_{Erk:MEK} + [Erk]} + k_{Erk:PP2A}[PP2A]\frac{[Erk^*]}{KM_{Erk:PP2A} + [Erk^*]}$$

$$\frac{d}{dt}[p90Rsk^*] = k_{p90Rsk:Erk}[Erk^*]\frac{[p90Rsk]}{KM_{p90Rsk:Erk} + [p90Rsk]} - k_{DSOS:p90Rsk}[p90Rsk^*]\frac{[SOS]}{KM_{DSOS:p90Rsk} + [SOS]}$$

$$\frac{d}{dt}[p90Rsk] = kd_{p90Rsk}[p90Rsk^*] - k_{p90Rsk:Erk}[Erk^*]\frac{[p90Rsk]}{KM_{p90Rsk:Erk} + [p90Rsk]}$$

$$\frac{d}{dt}[PIK3^*] = k_{PIK3:Ras}[Ras^*]\frac{[PIK3]}{KM_{PIK3:Ras} + [PIK3]} + k_{PIK3:IGF1R}[IGF1R^*]\frac{[PIK3]}{KM_{PIK3:IGF1R} + [PIK3]} + k_{PIK3:EGFR}[EGFR^*]\frac{[PIK3]}{KM_{PIK3:EGFR} + [PIK3]} - k_{Akt:PIK3}[Akt]\frac{[PIK3^*]}{KM_{Akt:PIK3} + [PIK3^*]}$$

$$\frac{d}{dt}[PIK3] = -k_{PIK3:Ras}[Ras^*]\frac{[PIK3]}{KM_{PIK3:Ras} + [PIK3]} - k_{PIK3:IGF1R}[IGF1R^*]\frac{[PIK3]}{KM_{PIK3:IGF1R} + [PIK3]} - k_{PIK3:EGFR}[EGFR^*]\frac{[PIK3]}{KM_{PIK3:EGFR} + [PIK3]} + kf_{PIK3} * [PIK3^*]$$

$$\frac{d}{dt}[Akt^*] = -k_{Raf:Akt}[Akt^*]\frac{[Raf^*]}{KM_{Raf:Akt} + [Raf^*]} + k_{Akt:PIK3}[Akt]\frac{[PIK3^*]}{KM_{Akt:PIK3} + [PIK3^*]}$$

$$\frac{d}{dt}[Akt] = -k_{Akt:PIK3}[Akt]\frac{[PIK3^*]}{KM_{Akt:PIK3} + [PIK3^*]} + kd_{Akt}[Akt^*].$$

Conservation lows:

$$[EGFR_{Tot}] = [EGFR^*] + [EGFR]$$

$$[IGF1R_{Tot}] = [IGF1R^*] + [IGF1R]$$

$$[SOS_{Tot}] = [SOS] + [DSOS]$$

$$[Ras_{Tot}] = [Ras^*] + [Ras]$$

$$[Raf_{Tot}] = [Raf^*] + [Raf]$$

$$[MEK_{Tot}] = [MEK^*] + [MEK]$$

$$[Erk_{Tot}] = [Erk^*] + [Erk]$$

$$[PIK3_{Tot}] = [PIK3^*] + [PIK3]$$

$$[Akt_{Tot}] = [Akt^*] + [Akt].$$

All the parameters of the model 7.

Variable	Definition	Value	Source
γ_{EGFR}	EGFR deactivation	0.02	(Orton et al., 2009)
$k_{SOS:E}$	Catalytic constant for SOS activation by EGFR	694.731	(Brown et al., 2004)
$KM_{SOS:E}$	Michaelis–Menten constant for SOS activation by EGFR	6086070.0	(Brown et al., 2004)
$k_{PIK3:EGFR}$	Catalytic constant for PIK3 activation by EGFR	10.6737	(Brown et al., 2004)
$KM_{PIK3:EGFR}$	Michaelis–Menten constant for PIK3 activation by EGFR	184912.0	(Brown et al., 2004)
γ_{IGF1R}	IGF1R deactivation	0.02	Parameters estimation
$k_{SOS:I}$	Catalytic constant for SOS activation by IGF1R	500.0	Parameter estimation
$KM_{SOS:I}$	Michaelis–Menten constant for SOS activation by IGF1R	1000000.0	Parameter estimation
$k_{PIK3:IGF1R}$	Catalytic constant for PIK3 activation by IGF1R	10.6737	Parameter estimation
$KM_{PIK3:IGF1R}$	Michaelis–Menten constant for PIK3 activation by IGF1R	184912.0	Parameter estimation
$k_{DSOS:p90Rsk}$	Catalytic constant for DSOS deactivation by p90Rsk	161197.0	(Brown et al., 2004)
$KM_{DSOS:p90Rsk}$	Michaelis–Menten constant for DSOS deactivation by p90Rsk	896896.0	(Brown et al., 2004)
$k_{Ras:SOS}$	Catalytic constant for Ras activation by SOS	32.344	(Brown et al., 2004)
$KM_{Ras:SOS}$	Michaelis–Menten constant for Ras activation by SOS	35954.3	(Brown et al., 2004)
$k_{Ras:RasGab}$	Catalytic constant for Ras deactivation by RasGab	1509.36	(Brown et al., 2004)
$KM_{Ras:RasGab}$	Michaelis–Menten constant for Ras deactivation by RasGab	1432410.0	(Brown et al., 2004)
$k_{Raf:Ras}$	Catalytic constant for Raf activation by Ras	0.884096	(Brown et al., 2004)
$KM_{Raf:Ras}$	Michaelis–Menten constant for Raf deactivation by Ras	62464.6	(Brown et al., 2004)
$k_{Raf:RafPP}$	Catalytic constant for Raf deactivation by RafPP	0.126329	(Brown et al., 2004)
$KM_{Raf:RafPP}$	Michaelis–Menten constant for Raf deactivation by RafPP	1061.71	(Brown et al., 2004)
$k_{Raf:Akt}$	Catalytic constant for Raf deactivation by Akt	15.1212	(Brown et al., 2004)
$KM_{Raf:Akt}$	Michaelis–Menten constant for Raf deactivation by Akt	119355.0	(Brown et al., 2004)
$k_{Raf:MEK}$	Catalytic constant for MEK activation by Raf	185.759	(Brown et al., 2004)
$KM_{Raf:MEK}$	Michaelis–Menten constant for MEK activation by Raf	4768350.0	(Brown et al., 2004)

(continued on next page)

(*continued*)

Variable	Definition	Value	Source
$k_{MEK:PP2A}$	Catalytic constant for MEK deactivation by PP2A	2.83243	(Brown et al., 2004)
$KM_{MEK:PP2A}$	Michaelis–Menten constant for MEK deactivation by PP2A	518753.0	(Brown et al., 2004)
$k_{Erk:MEK}$	Catalytic constant for ERK activation by MEK	9.85367	(Brown et al., 2004)
$KM_{Erk:MEK}$	Michaelis–Menten constant for ERK deactivation by MEK	1007340.0	(Brown et al., 2004)
$k_{Erk:PP2A}$	Catalytic constant for ERK activation by PP2A	9.85367	(Brown et al., 2004)
$KM_{Erk:PP2A}$	Michaelis–Menten constant for ERK deactivation by PP2A	1007340.0	(Brown et al., 2004)
kd_{p90Rsk}	p90Rsk deactivation	0.0050	(Orton et al., 2009)
$k_{p90Rsk:Erk}$	Catalytic constant for p90Rsk activation by Erk	0.0213697	(Brown et al., 2004)
$KM_{p90Rsk:Erk}$	Michaelis–Menten constant for p90Rsk activation by Erk	763523.0	(Brown et al., 2004)
$k_{Akt:PIK3}$	Catalytic constant for Akt activation by PIK3	0.0566279	(Brown et al., 2004)
$KM_{Akt:PIK3}$	Michaelis–Menten constant for Akt activation by PIK3	653951.0 1	(Brown et al., 2004)
kd_{Akt}	Akt deactivation	0.0050	(Orton et al., 2009)

Initial concentration of the species

Species	Value	Source
*EGFR**	8000	(Orton et al., 2009)
*IGF1R**	8000	(Orton et al., 2009)
SOS	120,000.0	(Orton et al., 2009)
DSOS	0	(Orton et al., 2009)
*Ras**	0	(Orton et al., 2009)
Ras	120,000	(Orton et al., 2009)
*Raf**	0	(Orton et al., 2009)
Raf	120,000	(Orton et al., 2009)
*MEK**	0	(Orton et al., 2009)
MEK	600,000	(Orton et al., 2009)
*Erk**	0	(Orton et al., 2009)
Erk	600,000	(Orton et al., 2009)
*p90Rsk**	0	(Orton et al., 2009)
p90Rsk	120,000	(Orton et al., 2009)
*PIK3**	0	(Orton et al., 2009)
PIK3	120,000	(Orton et al., 2009)
RafPP	120,000	(Orton et al., 2009)
PP2A	120,000	(Orton et al., 2009)
RasGab	120,000	(Orton et al., 2009)

References

Bader AG, Kang S, Zhao L, Vogt PK. Oncogenic pi3k deregulates transcription and translation. Nat Rev Cancer 2005;5(12):921–9.

Becker MA, Yee D. Egfr signaling networks in cancer therapy (chapter 11). Business 2008:155–68.

Bianconi F. Dynamic modeling, parameter estimation and experiment design in Systems Biology with applications to Oncology. Ph.D. thesis. University of Perugia; 2010.

Bianconi F, Lillacci G, Valigi P. Dynamic modeling and parameter identification for biological networks: application to the DNA damage and repair processes. In: Liu LA, Wei D, Li Y, editors. Handbook of research on computational and systems biology: interdisciplinary applications; 2010.

Blakesley V, Stannard B, Kalebic T, et al. Role of the IGF-I receptor in mutagenesis and tumor promotion. J Endocrinol 1997;152:339–44.

Boguski M, McCormick F. Proteins regulating ras and its relatives. Nature 1993;366 (6456):643–54.

Brown KS, Hill CC, Calero Ga, Myers CR, Lee KH, Sethna JP, et al. The statistical mechanics of complex signaling networks: nerve growth factor signaling. Physical Biology 2004;1(3–4):184–95.

Citri A, Skaria KB, Yarden Y. The deaf and the dumb: the biology of ERBB-2 and erbb-3. Experimental Cell Research 2003;284(1):54–65.

Denley A, Cosgrove LJ, Booker GW, Wallace JC, Forbes BE. Molecular interactions of the IGF system. Cytokine & Growth Factor reviews 2005;16(4–5):421–39.

Dong Chen, Waters SB, Holt KH, Pessin JE. Sos phosphorylation and disassociation of the grb2–sos complex by the erk and jnk signaling pathways. The Journal of biological chemistry 1996;271(11):6328–32.

Dufourny B, Alblas J, vanTeeffelen H, et al. Mitogenic signaling of insulin-like growth factor i in mcf-7 human breast cancer cells requires phosphatidylinositol 3-kinase and is independent of mitogen-activated protein kinase. J Biol Chem 1997;272: 31163–71.

Dziadziuszko R, Merrick D, Witta S, Mendoza A, Szostakiewicz B, Szymanowska A, et al. Insulin-like growth factor receptor 1 (IGF1R) gene copy number is associated with survival in operable non-small-cell lung cancer: a comparison between igf1r fluorescent in situ hybridization, protein expression, and mrna expression. J Clin Onco 2010;28(13):2174–80.

Frödin M, Gammeltoft S. Role and regulation of 90 kda ribosomal s6 kinase (rsk) in signal transduction. Molecular and Cellular Endocrinology 1999;151(1–2):6.

Gary L, Johnson RL. Mitogen-activated protein kinase pathways mediated by erk, jnk, and p38 protein kinases. Science 2002;298(5600):1911–2.

Gong Y, Yao E, Shen R, Goel A, Arcila M, Teruya-Feldstein J, et al. High expression levels of total igf-1r and sensitivity of nsclc cells in vitro to an anti-igf-1r antibody (r1507). PloS one 2009;4(10):e7273.

Gonzalez-Angulo AM, Hennessy BTJ, Mills GB. Future of personalized medicine in oncology: A systems biology approach. Journal of clinical oncology: official journal of the American Society of Clinical Oncology 2010;28(16):2777–83.

Gualberto A, Dolled-Filhart M, Gustavson M, Christiansen J, Wang Y, Hixon M, et al. Molecular analysis of non-small cell lung cancer identifies subsets with different sensitivity to insulin-like growth factor i receptor inhibition. Clin Cancer Res 2010;16(18):4654–65.

Guan KL, Figueroa C, Brtva TR, Zhu T, Taylor J, Barber TD, et al. Negative regulation of the serine/threonine kinase b-raf by akt. The Journal of Biological Chemistry 2000;275 (35):27354–9.

Hennessy BT, Smith DL, Ram PT, Lu Y, Mills GB. Exploiting the pi3k/akt pathway for cancer drug discovery. Nat Rev Drug Discov 2005;4(12):988-1004.

Hindmarsh AC, Brown PN, Grant KE, Lee SL, Serban R, Shumaker DE, et al. Sundials: suite of nonlinear and differential/algebraic equation solvers. ACM Trans Math Softw 2005;31(3):363–96.

Jiang Y, Rom WN, Yie Ta, Chi CX, Tchou-Wong KM. Induction of tumor suppression and glandular differentiation of a549 lung carcinoma cells by dominant-negative igf-i receptor. Oncogene 1999;18(44):6071–7.

Jones JI, Clemmons DR. Insulin-like growth factors and their binding proteins: biological actions. Endocr Rev 1995;16(1):3-34.

Khandwala H, McCutcheon I, Flyvbjerg A, Friend K. The effects of insulin-like growth factors on tumorigenesis and neoplastic growth. Endocr Rev 2000;21:215–44.

Kim EK, Choi EJ. Pathological roles of mapk signaling pathways in human diseases. Biochimica et Biophysica Acta 2010;1802(4):396–405.

Lazebnik Y. Can a biologist fix a radio? — or, what I learned while studying apoptosis. Cancer cell 2002;2(3):179–82.

LeRoith D, Werner H, Beitner-Johnson D, Roberts CT. Molecular and cellular aspects of the insulin-like growth factor i receptor. Endocr Rev 1995;16(2):143–63.

López-Calderero I, Chávez ES, García-Carbonero R. The insulin-like growth factor pathway as a target for cancer therapy. Clinical and Translational Oncology 2010;12 (5):326–38.

Ludovini V, Bellezza G, Pistola L, Bianconi F, Di Carlo L, Sidoni a, et al. High co-expression of both insulin-like growth factor receptor-1 (igfr-1) and epidermal growth factor

receptor (egfr) is associated with shorter disease-free survival in resected non-small-cell lung cancer patients. Annals of Oncology: official Journal of the European Society for Medical Oncology/ESMO 2009;20(5):842–9.
Ludovini V, Bianconi F, Pistola L, Chiari R, Minotti V, Colella R, et al. Phosphoinositide-3-kinase catalytic alpha and kras mutations are important predictors of resistance to therapy with epidermal growth factor receptor tyrosine kinase inhibitors in patients with advanced non-small cell lung cancer. J Thorac Oncol 2011. Epub ahead of print.
Markevich NI, Hoek JB, Kholodenko BN. Signaling switches and bistability arising from multisite phosphorylation in protein kinase cascades. The Journal of Cell Biology 2004;164(3).
Mendelsohn J, Baselga J. Epidermal growth factor receptor targeting in cancer. Semin Oncol 2006;33(4):369–85.
Mitsudomi T, Yatabe Y. Epidermal growth factor receptor in relation to tumor development: Egfr gene and cancer. FEBS J 2010;277(2):301–8.
Orton RJ, Adriaens ME, Gormand A, Sturm OE, Kolch W, Gilbert DR. Computational modelling of cancerous mutations in the egfr/erk signalling pathway. BMC Syst Biol 2009;3:100.
Pearson G. Mitogen-activated protein (map) kinase pathways: regulation and physiological functions. Endocr Rev 2001;22(2):153–83.
Qi M, Elion Ea. Map kinase pathways. Journal of cell science 2005;118(Pt 16):3569–72.
Riedemann J, Macaulay VM. Igf1r signalling and its inhibition. Endocrine-related cancer 2006;13(Suppl 1):S33–43.
Roberts PJ, Der CJ. Targeting the raf–mek–erk mitogen-activated protein kinase cascade for the treatment of cancer. Oncogene 2007;26(22):3291–310.
Scaltriti M, Baselga J. The epidermal growth factor receptor pathway: a model for targeted therapy. Clinical Cancer Research 2006;12(18):5268–72.
Schlessinger J. Ligand-induced, receptor-mediated dimerization and activation of egf receptor. Cell 2002;110(6):669–72.
Schubbert S, Shannon K, Bollag G. Hyperactive ras in developmental disorders and cancer. Nat Rev Cancer 2007;7(4):295–308.
Shane Donovana KMS, Bollagb G. Gtpase activating proteins: critical regulators of intracellular signaling. Biochimica et Biophysica Acta (BBA) — Reviews on Cancer 2002;1602(1):23–45.
Varella-Garcia M, Diebold J, Eberhard DA, Geenen K, Hirschmann A, Kockx M, et al. Egfr fluorescence in situ hybridisation assay: guidelines for application to non-small-cell lung cancer. Journal of Clinical Pathology 2009;62(11):970–7.
Vivanco I, Sawyers CL. The phosphatidylinositol 3-kinase–akt pathway in human cancer. Nat Rev Cancer 2002;2(7):489–501.
Yarden Y. The egfr family and its ligands in human cancer. signalling mechanisms and therapeutic opportunities. (Oxford, England: 1990)European journal of cancer 2001;37(Suppl 4):S3–8.
Yoon S, Seger R. The extracellular signal-regulated kinase: multiple substrates regulate diverse cellular functions. Growth Factors 2006;24:21–44.
Zandi R, Larsen AB, Andersen P, Stockhausen MT, Poulsen HS. Mechanisms for oncogenic activation of the epidermal growth factor receptor. Cell Signal 2007;19(10):2013–23.
Zielinski R, Przytycki P, Zheng J, Zhang D, Przytycka T, Capala J. The crosstalk between egf, igf, and insulin cell signaling pathways — computational and experimental analysis. BMC Syst Biol 2009;3(1):88. Crosstalk between EGF, IGF.